AFFDL-TR-74-5

A SPECTRUM TRUNCATION AND DAMAGE TOLERANCE STUDY ASSOCIATED WITH THE C-5A OUTBOARD PYLON AFT TRUSS LUGS

J. P. GALLAGHER
H. D. STALNAKER
J. L. RUDD

TECHNICAL REPORT AFFDL—TR—74—5

MAY 1974

AIR FORCE FLIGHT DYNAMICS LABORATORY
AIR FORCE SYSTEMS COMMAND
WRIGHT—PATTERSON AIR FORCE BASE, OHIO 45433

NOTICE

When Government drawings, specifications, or other data are used for any purpose other than in connection with a definitely related Government procurement operation, the United States Government thereby incurs no responsibility nor any obligation whatsoever; and the fact that the government may have formulated, furnished, or in any way supplied the said drawings, specifications, or other data, is not to be regarded by implication or otherwise as in any manner licensing the holder or any other person or corporation, or conveying any rights or permission to manufacture, use, or sell any patented invention that may in any way be related thereto.

This report has been reviewed and is approved for publication.

FRANCIS J. JANIK, JR
Chief, Solid Mechanics Branch
Structures Division

Copies of this report should not be returned unless return is required by security considerations, contractual obligations, or notice on a specific document.

AIR FORCE/56780/26 July 1974 — 300

UNCLASSIFIED

SECURITY CLASSIFICATION OF THIS PAGE *(When Data Entered)*

REPORT DOCUMENTATION PAGE		READ INSTRUCTIONS BEFORE COMPLETING FORM
1. REPORT NUMBER AFFDL-TR-74-5	2. GOVT ACCESSION NO.	3. RECIPIENT'S CATALOG NUMBER
4. TITLE *(and Subtitle)* A SPECTRUM TRUNCATION AND DAMAGE TOLERANCE STUDY ASSOCIATED WITH THE C-5A OUTBOARD PYLON AFT TRUSS LUGS		5. TYPE OF REPORT & PERIOD COVERED 6. PERFORMING ORG. REPORT NUMBER
7. AUTHOR*(s)* J. P. Gallagher H. D. Stalnaker J. L. Rudd		8. CONTRACT OR GRANT NUMBER*(s)*
9. PERFORMING ORGANIZATION NAME AND ADDRESS Air Force Flight Dynamics Laboratory Wright-Patterson Air Force Base, Ohio		10. PROGRAM ELEMENT, PROJECT, TASK AREA & WORK UNIT NUMBERS Project 410A0504
11. CONTROLLING OFFICE NAME AND ADDRESS		12. REPORT DATE May 1974 13. NUMBER OF PAGES 52
14. MONITORING AGENCY NAME & ADDRESS*(if different from Controlling Office)*		15. SECURITY CLASS. *(of this report)* UNCLASSIFIED 15a. DECLASSIFICATION/DOWNGRADING SCHEDULE

16. DISTRIBUTION STATEMENT *(of this Report)*

Approved for public release; distribution unlimited.

17. DISTRIBUTION STATEMENT *(of the abstract entered in Block 20, if different from Report)*

18. SUPPLEMENTARY NOTES

19. KEY WORDS *(Continue on reverse side if necessary and identify by block number)*

Load Spectrum Truncation

Fracture Mechanics

Fatigue Crack Propagation

20. ABSTRACT *(Continue on reverse side if necessary and identify by block number)*

A simplified lug specimen configuration is subjected to two load spectra derived from the same exceedance data: (1) a 17 level block loading program, and (2) a 14-mission flight-by-flight loading program. Crack growth data from the two spectra for this PH 13-8Mo material are compared on a life basis; each spectrum contained an equal number of Ground Air Ground (GAG) cycles per lifetime. An analysis of the effect associated with the degree of truncation

DD FORM 1 JAN 73 1473 EDITION OF 1 NOV 65 IS OBSOLETE

UNCLASSIFIED

SECURITY CLASSIFICATION OF THIS PAGE *(When Data Entered)*

to which the flight by flight spectrum could be subjected was performed using the conservative no retardation - no load interaction crack growth model and the Willenborg crack growth retardation model. The stress intensity factor calibration developed using finite element techniques is supplemented with stress intensity factor values obtained using the Anderson - James inverse approach. Additional tests on 7075-T6 aluminum are described which investigate the importance of load redundancy.

FOREWORD

At the request of ASD/ENF and the C-5A Systems Program Office, the Air Force Flight Dynamics Laboratory conducted this test and analysis program under Project No. 410A0504. J. P. Gallagher served as the Project Engineer for this work. The testing was accomplished in Bldg 65 of the Experimental Branch, Structures Division; Messrs. W. Soward and O. B. Jarrels were responsible for most of the crack length readings.

Work was accomplished during the time period December 1972 to September 1973. This report was submitted by the authors in October 1973.

TABLE OF CONTENTS

FIGURES

TABLES

SECTION I

INTRODUCTION

In late 1972, a C-5A outboard engine pylon aft truss lug (see Figure 1 for geometry and critical section) failed during a full-scale fatigue test at the contractor's facility. While the lug section failed after approximately 42 block load applications (equivalent to 1.75 lifetimes), the failure excited immediate Air Force interest because it occurred during the first series of equivalent engine run-up load cycles following a tear-down inspection in which no cracks were found (Reference 1).

At the request of Aeronautical Systems Division (ASD/ENF), the C-5A System Project Office, and the C-5A Independent Review Team (IRT), the Air Force Flight Dynamics Laboratory initiated fatigue crack growth tests on laboratory specimens simulating the lug configuration. These specimens were fabricated from material identical to that used in the hardware. There were two objectives for conducting the fatigue studies on precracked specimens: (1) to determine if failures could be achieved in approximately the same number of cycles as noted for the full-scale fatigue test failure, and (2) to provide data for extrapolating test results to flying aircraft.

Upon completion of the original series of tests, a follow-on test and analysis program was initiated to investigate (1) the influence of the lower level loads in the flight-by-flight test spectrum, and (2) the damage tolerance of parallel loaded lug elements.

This report describes the test details associated with the requested fatigue test program, a discussion of these results, an analysis approach which is considered useful for determining the influence of the low load level truncation in flight-by-flight spectra, and the application of the Anderson - James inverse stress intensity factor analysis (see Appendix).

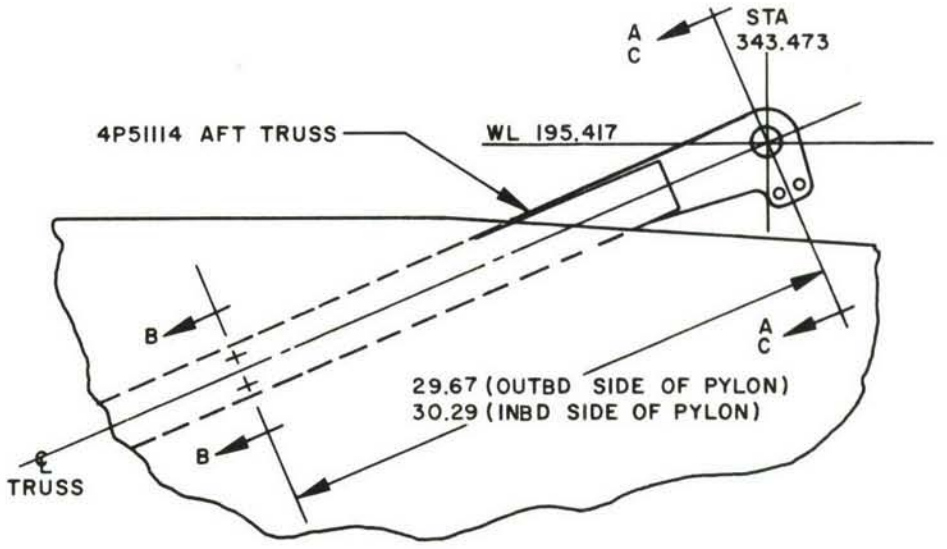

OUTBOARD PYLON
(VIEW LOOKING INBOARD)
CRITICAL SECTIONS I, Ia & Ib

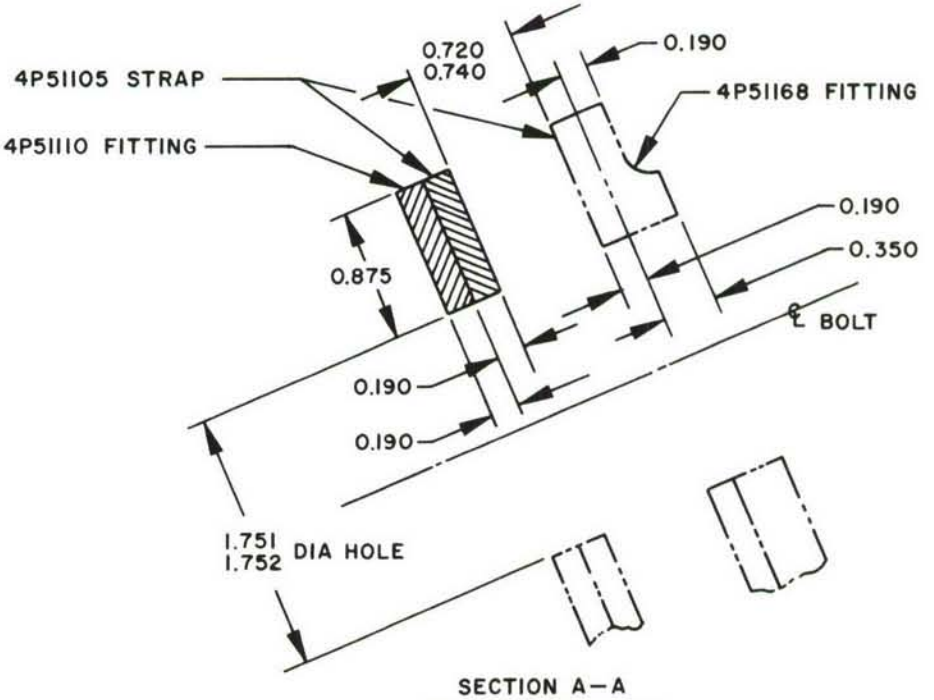

SECTION A—A
CRITICAL SECTION I

Figure 1. C-5A Outboard Pylon Aft Truss with Section To Be Modeled

SECTION II

TEST INFORMATION

1. TEST SPECIMEN GEOMETRY AND MATERIALS

For each of the C-5A spectra considered, two links of the type shown in Figure 2 were tested in parallel in the configuration illustrated in Figure 3. The two-precracked-link configuration was suggested by the C-5A IRT as an appropriate model for the loading and for the lug geometry shown in Figure 1. The links were manufactured from a PH 13-8 Mo steel which was subjected to a 1000°F heat treatment. A jeweler's saw was used to introduce a small notch (0.012 inch deep, 0.005 inch wide) at one edge of a lug hole. Constant amplitude loading (minimum load = 5 kip, maximum load = 25 kip) was applied to two links loaded in parallel to develop the starter cracks at the base of the small notches.

For one phase of the follow-on program, the links associated with the Anderson-James Inverse Stress Intensity Factor program (see Appendix) were manufactured from 7075-T6 (0.190 inch thick) Aluminum. When four aluminum links were placed in parallel, an uncracked link was positioned adjacent to a cracked link. The uncracked - cracked units (shown in Figure 3C) were substituted for the single link units shown in Figure 3B. The cracked link was positioned on the outside of each two-link (cracked-uncracked) unit for the convenience of the observers (e.g., link A and link B in Figure 3C).

The zero-tension crack growth rate data plotted in Figure 4 for PH 13-8 Mo steel can be used in analyzing crack growth behavior under either the block or flight-by-flight load spectra considered in this investigation. Three data sets [2, 3, and 4] are given for comparison.

2. TEST SPECTRA

The 17 level block load spectrum applied to one set of two cracked parallel PH 13-8 MO steel link specimens is listed in Table I. The major loads in this block spectrum are the ground-air-ground (GAG),

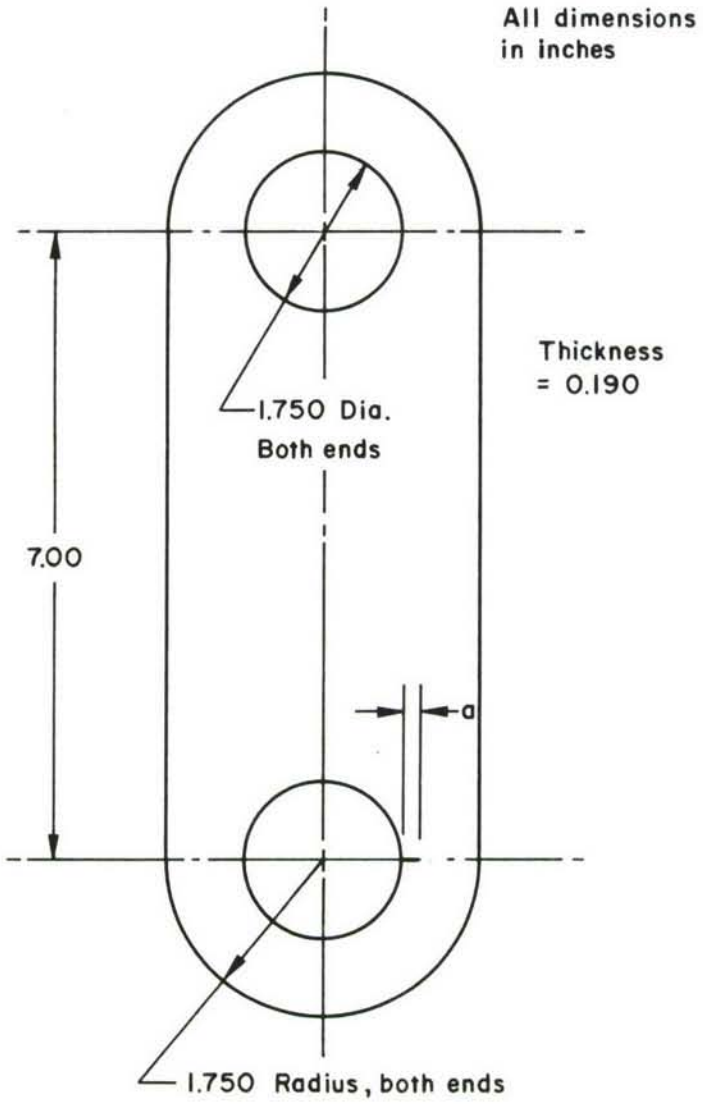

Figure 2. Dimensions of Link Specimens

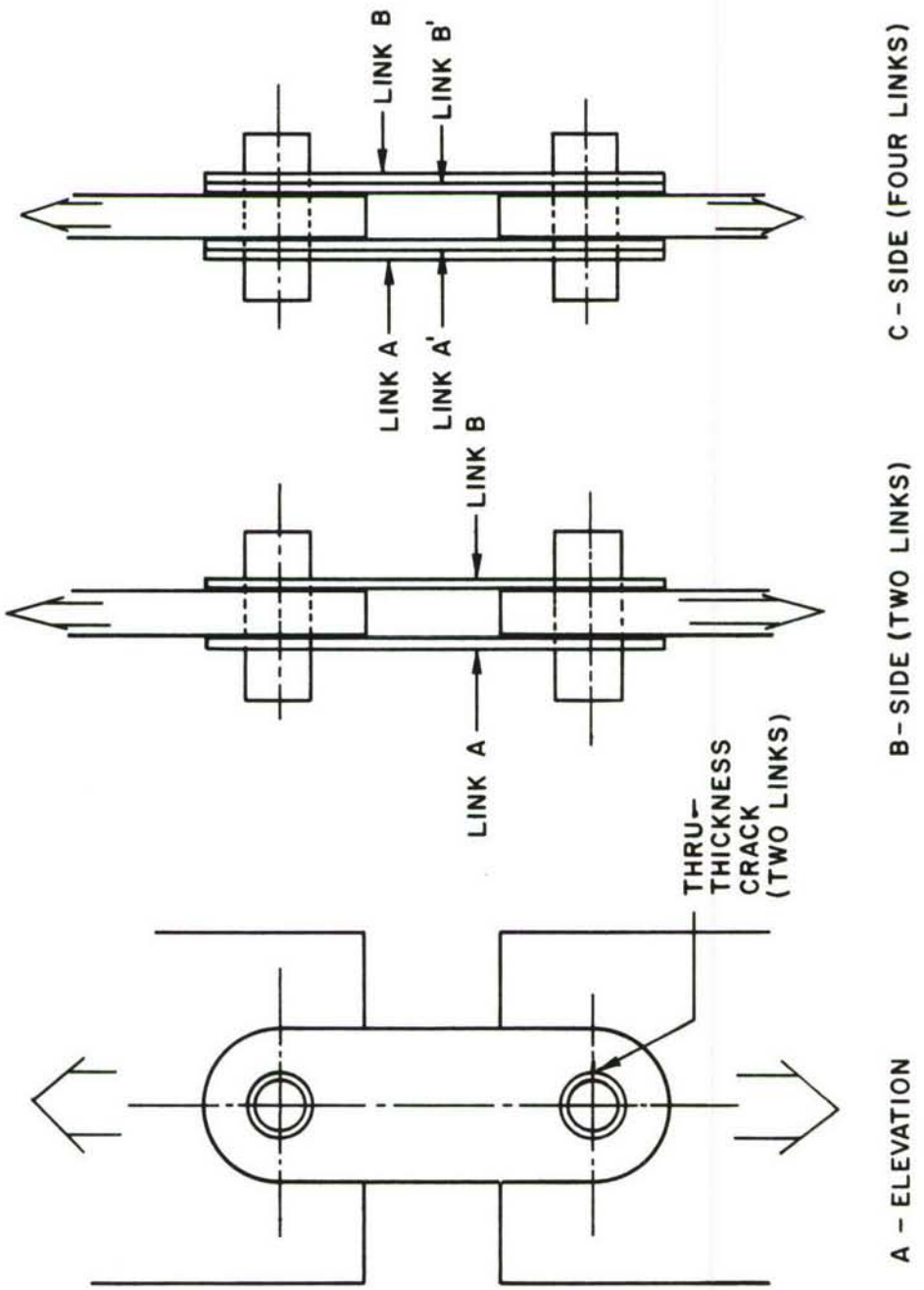

Figure 3. Configuration of Test Specimens

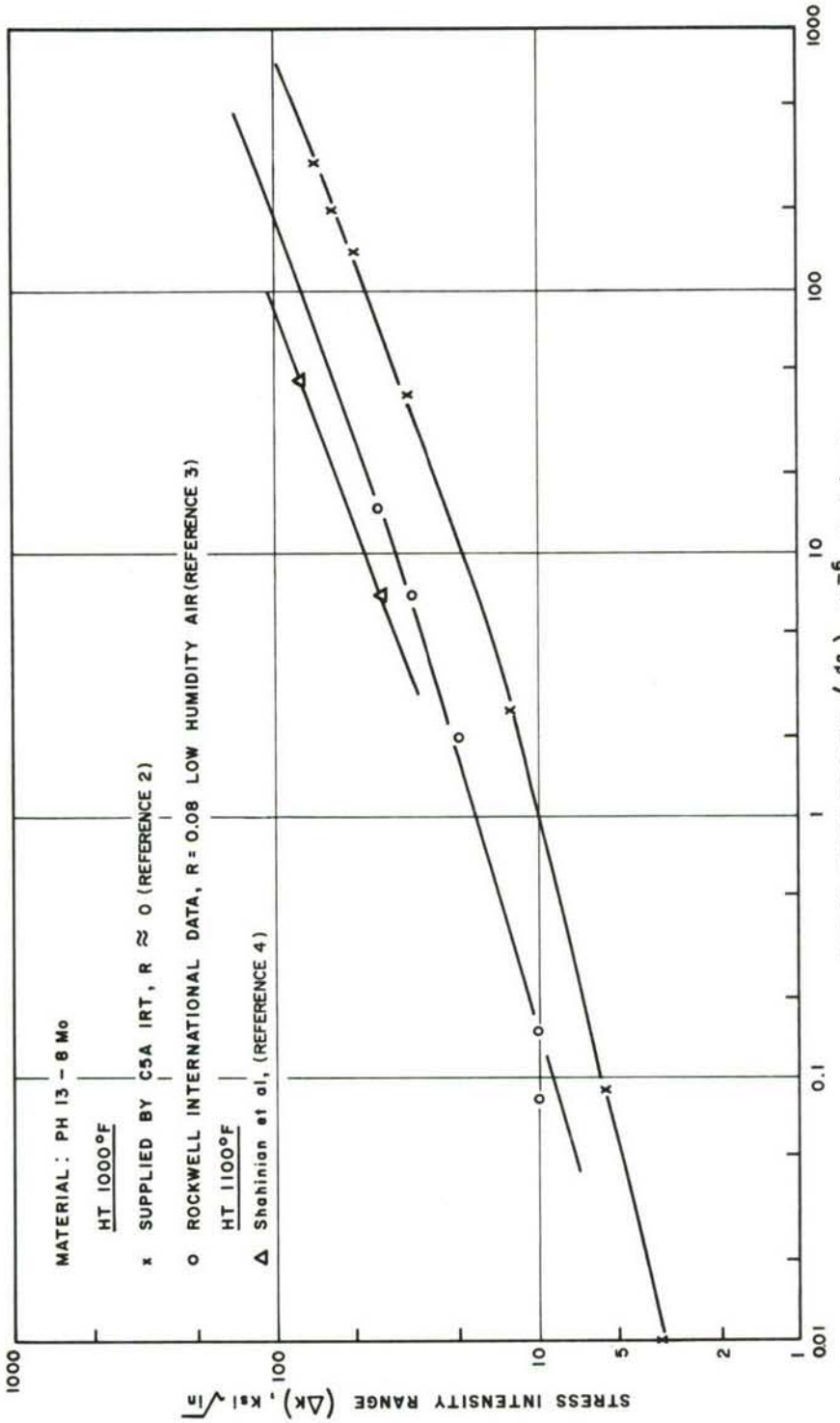

Figure 4. Fatigue Crack Growth Behavior of PH 13-8 Mo Steel

TABLE I

PYLON NO. 7 BLOCK TEST SPECTRUM*
DERIVED FROM TRM-P DATED 7 DECEMBER 1972

Loading Applied in Block	Condition	Cycles at 5 Hz	Max Load ** Kip	Min Load ** Kip
B	F1A	1	8.23	1.16
A,B	F1B	10	6.99	2.40
B	F1B	2	6.99	2.40
A,B	F1C	898	5.85	3.50
B	F2A	1	7.04	1.73
A,B	F2B	17	6.23	2.49
B	F2B	3	6.23	2.49
A,B	F2C	1540	5.45	3.32
B	F3A	1	7.63	2.68
A,B	F3B	8	6.93	3.38
B	F3B	4	6.93	3.38
A,B	F3C	2790	6.09	4.27
A,B	F4A	5600	5.43	4.27
A,B	FG1	3832	4.81	.10
A,B	FG2	160	8.14	.10
A,B	FG3	8	11.55	.10
B	FG4	2	15.05	.10
A,B	GAG	303	37.92	.20
A,B	TAG	178	28.61	.10
A,B	ERU	303	31.18	.10

* Spectrum = 5 (4A+B) = 1 Lifetime
B block is growth of A block

** Divide loads by 0.664 to obtain the bearing stress (also the net section stress) on one link.

touch and go (TAG), and engine run up (ERU) loads. Table I indicates that a decomposition of the main load spectrum was made to accommodate the fractional cycles per block. All fractional cycles were collected and applied in block B, which was applied after every four applications of block A. Note that block B also contains all load levels contained in block A.

The 14 mission flight-by-flight load spectrum applied to the second set of PH 13-8 Mo steel link specimens is provided by Table II. This load spectrum can be broken down into two basic recurring flights - the GAG (Full-Stop Landings) and the TAG type flights. Both GAG and TAG flights incorporate the influence of infrequently occurring loads by adding additional cycles to the basic flight on a one per tenth, one per hundredth, and one per thousandth recurrence of the basic flight. The GAG and TAG type flights are proportioned so that 10 GAG flights occur for every 6 TAG flights. Using the notation of Table II, the flights were arranged according to the order in the following equation:

$$\begin{aligned} \text{Spectrum} = {} & 9\boxed{A} + \boxed{B} + 6\boxed{E} + 9\boxed{A} + \boxed{B} + 3\boxed{E} + \\ & + \boxed{F} + 2\boxed{E} + 9\boxed{A} + \boxed{B} + 6\boxed{E} + 9\boxed{A} + \\ & + \boxed{B} + \boxed{E} + \boxed{F} + 4\boxed{E} + \cdots \end{aligned} \qquad (1)$$

where $\boxed{A}$ is the basic GAG flight, $\boxed{B}$ is the one per tenth GAG flight (it includes all block $\boxed{A}$ loads), $\boxed{E}$ is the basic TAG flight, and $\boxed{F}$ is the one per tenth TAG flight (it includes all block $\boxed{E}$ loads). Flight Blocks $\boxed{C}$, $\boxed{D}$, $\boxed{G}$ and $\boxed{H}$ are included when Equation 1 is carried out to include a sufficiently large number of flights; Blocks $\boxed{C}$, $\boxed{D}$, $\boxed{G}$ and $\boxed{H}$ represent the one per hundredth GAG flight, the one per thousandth GAG flight, the one per hundredth TAG flight and the one per thousandth TAG flight, respectively. There are 7572 GAG flights and 4543 TAG flights in this spectrum lifetime (1 Lifetime = 12,115 flights).

TABLE II

PYLON NO. 7 FLIGHT-BY-FLIGHT TEST SPECTRUM
DERIVED FROM TRM-P DATED 7 DEC 1972

There are 7572 Full-Stop Landing (FSL) Flights Applied in a Lifetime:
1 Average Flight = 5.38 Flight Hrs.

GAG (FSL) Spectrum Description
A = Every flight basic GAG spectrum
B = 1 in 10 GAG spectrum
C = 1 in 100 GAG spectrum
D = 1 in 1000 GAG spectrum

D block is growth of C block, which is growth of B block, which is growth of A block.

TAG Spectrum Description
E = Every flight basic TAG spectrum
F = 1 in 10 TAG spectrum
G = 1 in 100 TAG spectrum
H = 1 in 1000 TAG spectrum

H block grows from G Block, which grows from F block, which grows from E block.

Order of Application
Spectrum = x (10A + 6E) subject to every tenth occurrence of each A or E, substitute B or F respectively; every hundredth substitute C or G respectively; and every thousandth, substitute D or H respectively.

GAG (FSL) SPECTRUM LOADS

Loading Applied in Blocks	Condition	Cycles at 5 Hz	Max Load ** Kip	Min Load ** Kip
B,C,D	1	2	31.3	.1
A,B,C,D	2	63	4.5	3.5
A,B,C,D	3	42	5.6	2.4
A,B,C,D	4	11	6.6	1.4
A,B,C,D	5	3	7.7	.3
A,B,C,D	6	1	8.8	.0
B,C,D	7	3	9.8	.0
B,C,D	8	2	10.9	.0
B,C,D	9	1	12.0	.0
C,D	10	6	13.0	.0
C,D	11	4	14.1	.1
C,D	12	3	15.1	.1
C,D	13	2	16.2	.0
C,D	14	2	17.3	.1
C,D	15	1	18.3	.1
D	16	9	19.4	.0

TABLE II (Contd)

Loading Applied in Blocks	Condition	Cycles at 5 Hz	Max Load ** Kip	Min Load ** Kip
D	17	6	20.5	.1
D	18	4	21.5	.1
D	19	3	22.6	.0
D	20	2	23.6	.0
D	21	1	24.7	.1
A,B,C,D	22	1	36.8	.0
A,B,C,D	23	7578*	4.5*	3.5*
A,B,C,D	24	914	5.6	2.4
A,B,C,D	25	251	6.6	1.4
A,B,C,D	26	83	7.7	.3
A,B,C,D	27	31	8.8	.0
A,B,C,D	28	12	9.8	.0
A,B,C,D	29	5	10.9	.1
A,B,C,D	30	2	12.0	.0
A,B,C,D	31	1	13.0	.0
B,C,D	32	5	14.1	.1
B,C,D	33	2	15.1	.1
B,C,D	34	1	16.2	.0
C,D	35	5	17.3	.1
C,D	36	3	18.3	.1
C,D	37	2	19.4	.0
C,D	38	1	20.5	.1
D	39	7	21.5	.1
D	40	5	22.6	.0
D	41	4	23.6	.0
D	42	3	24.7	.1
D	43	2	25.3	.0
D	44	2	26.8	.0
D	45	1	27.9	.1
D	46	1	29.0	.0

* Eliminated for Truncated Flight-by-Flight Spectrum

** Divide loads by 0.664 to obtain the bearing stress (also the net section stress) on one link.

TABLE II (Contd)

TAG SPECTRUM LOADS

Loading Applied in Blocks	Condition	Cycles at 5 Hz	Max Load ** Kip	Min Load ** Kip
A,B,C,D	1	1	4.5	3.5
A,B,C,D	2	1	27.4	0
A,B,C,D	3	1410*	4.5*	3.5*
A,B,C,D	4	169	5.6	2.4
A,B,C,D	5	46	6.6	1.4
A,B,C,D	6	15	7.7	.3
A,B,C,D	7	6	8.8	.0
A,B,C,D	8	2	9.8	.0
A,B,C,D	9	1	10.9	.1
B,C,D	10	4	12.0	.0
B,C,D	11	2	13.	.0
B,C,D	12	1	14.1	.1
C,D	13	4	15.1	.1
C,D	14	2	16.2	.0
D	15	8	17.3	.1
D	16	5	18.3	.1
D	17	3	19.4	.0
D	18	2	20.5	.1
D	19	1	21.5	.1
D	20	1	22.6	.0
D	21	1	23.6	.0

* Eliminated for truncated flight-by-flight spectrum.

** Divide loads by 0.664 to obtain the bearing stress (also the net section stress) on one link.

A truncated flight-by-flight spectrum based on the 14-mission spectrum was developed to study the influence of low level loads on growth behavior. Both GAG and TAG flights were modified by deleting a large quantity of cycles which occurred at the same (small) load level. In the GAG flight, 7578 cycles of the 3.5 to 4.5 kip loading were deleted; in the TAG flight, 1410 cycles at this load level were removed. (These deleted cycles are asterisked in Table II.)

3. TEST EQUIPMENT

A closed-loop, servocontrolled mechanical test system with a 100 kip static/50 kip dynamic load capability was employed to axially load the parallel set of links. The command signals (i.e., the spectrum loads) were stored in a 4096 byte memory digital programmer and then fed to a load servocontroller. The feedback signals were supplied by a load cell placed in series with the test specimens. The test spectra were run at a frequency of 5 Hz with the exception of the truncated flight-by-flight test spectrum, which was run at 2.5 Hz. The crack growth tests of the PH 13-8 Mo steel link specimens were conducted in a distilled water environment.

SECTION III

FATIGUE TEST RESULTS AND DISCUSSION

1. BLOCK SPECTRUM CRACKING BEHAVIOR

The block spectrum crack growth data (Links 1A and 1B), which are tabulated in Table III, are also plotted as a function of applied blocks in Figure 5. Each block represents 4 percent of a spectrum lifetime, and this equality has been used in Figure 5 to portray the crack length associated with a given percent aircraft life. Figure 5 shows that, while one crack was substantially longer than the other, the rates of cracking between 8 and 28 percent life were approximately the same. When the longer crack reached the edge of its link, crack growth increases in the second link, so that the crack reaches its link edge within an additional 7 percent of the lifetime. The links fractured during GAG cycle loading.

2. FLIGHT-BY-FLIGHT SPECTRUM CRACKING BEHAVIOR

All flight-by-flight crack growth data are listed in Table IV. The first 755 flights applied to Links 2A and 2B were associated with the untruncated 14-mission flight-by-flight test spectrum. The resulting crack growth data for the first 755 flights were plotted in Figure 6 and compared on a life basis with the crack growth behavior of Link 1B, which was subjected to the block load test.

To provide a curve which approximated the flight-by-flight data, the lifetime percentages associated with given crack lengths for Link 1B were multiplied by a factor of 0.8, (estimated on the basis of data presented in Figure 6). Scaling of crack growth behavior in this way is only justified when the following conditions are met: the geometry and material of the parts are the same so that the stress intensity factor calibration and basic crack growth response are identical; and the character of the spectra applied are similar in that the corresponding major loads control the crack growth behavior.

TABLE III

PYLON NO. 7 BLOCK TEST SPECTRUM CRACK GROWTH DATA

Specimen / Block Reading	1A (inch)	1B (inch)	o/o Life
0	0.065	0.028	0
*PREGAG	0.082	0.032	
POSTGAG	0.138	0.042	
PREGAG	0.138	0.042	
PRETAG	0.201	0.047	
PRE ERU	0.201	0.047	
1	0.225	0.051	4
PREGAG	0.225	0.052	
POSTGAG	0.255	0.064	
2	0.274	0.069	8
PREGAG	0.275	0.070	
POSTGAG	0.295	0.085	
3	0.310	0.105	12
PREGAG		0.115	
POSTGAG		0.122	
4	0.320	0.141	16
PREGAG	0.325	0.147	
POSTGAG	0.345	0.181	
5	0.373	0.205	20
PREGAG	0.385	0.212	
POSTGAG	0.401	0.219	
6	0.465	0.238	24
PREGAG	0.470	0.239	
POSTGAG	0.490		
7	0.570	0.285	28
PREGAG	0.580	0.285	
POSTGAG	0.660	0.297	
8	Crack to Edge	0.327	32
PREGAG	0.875	0.340	
POSTGAG	0.875	0.525	
9	0.875	0.589	36
PREGAG	0.875	0.602	
During the 293 Cycle of GAG		Crack to Edge 0.875	40

*303 GAG Cycles applied twice. Initial zero block crack lengths for 1A & 1B adjusted to 0.121 and 0.038 inch, respectively.

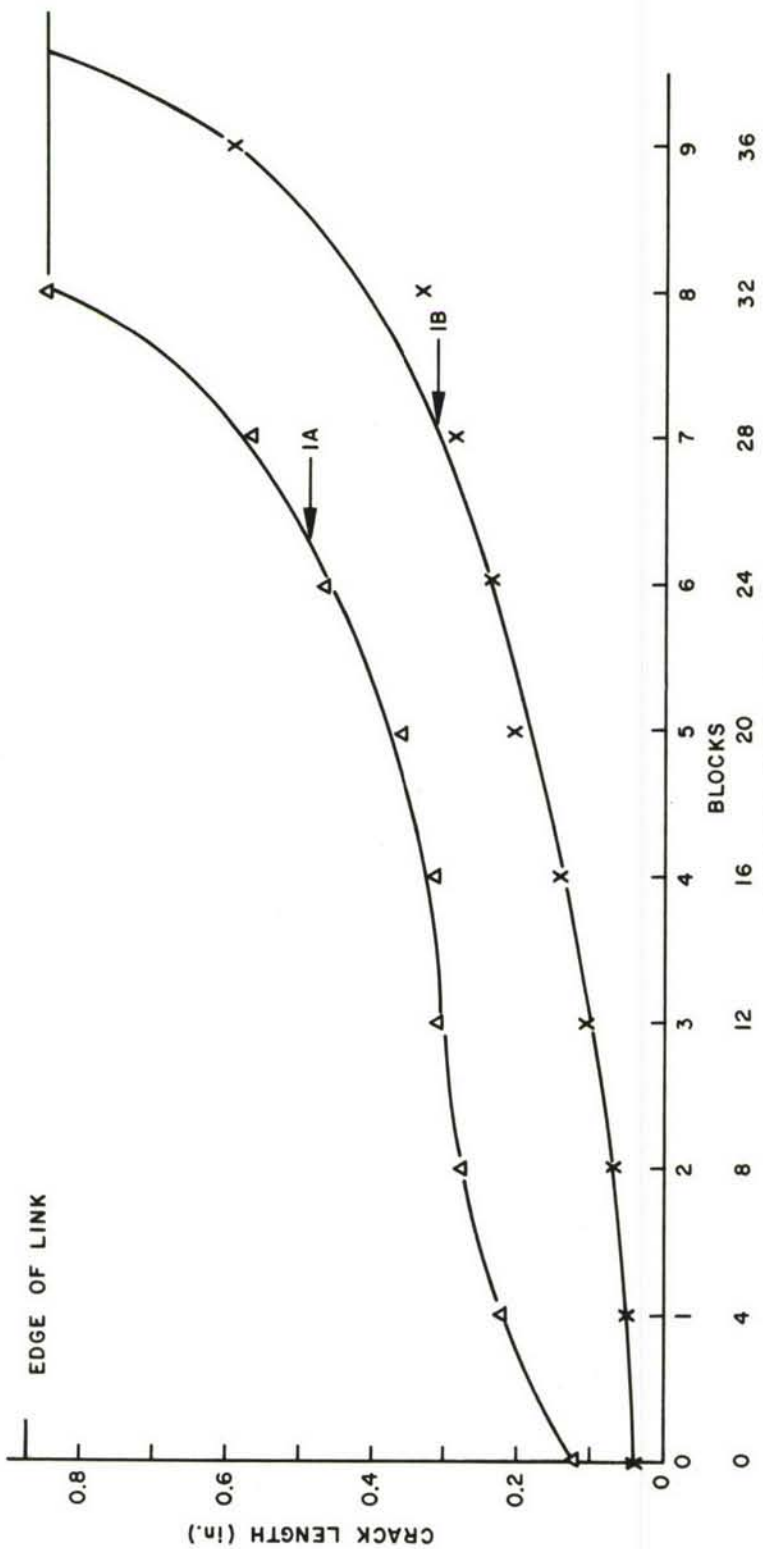

Figure 5. Block Spectrum Results - C-5A Pylon Aft Truss Lug Model

TABLE IV

PYLON NO. 7 FLIGHT-BY-FLIGHT TEST SPECTRUM CRACK GROWTH DATA

Specimen Total Flights Elapsed	Crack Length 2A (inch)	Crack Length 2B (inch)	Percent Lifetime (12,115)
0	0.033	0.033	0
42	0.041	0.037	0.35
80	0.048	0.039	0.66
122	0.049	0.040	1.01
170	0.052	0.042	1.40
220	0.052	0.043	1.82
250	0.053	0.043	2.06
282	0.055	0.044	2.33
330	0.056	0.046	2.73
362	0.056	0.046	2.99
410	0.059	0.046	3.38
442	0.065	0.047	3.65
490	0.066	0.047	4.04
522	0.069	0.047	4.31
570	0.071	0.049	4.70
602	0.072	0.050	4.97
650	0.075	0.051	5.36
682	0.077	0.054	5.63
730	0.089	0.057	6.02
755	0.089	0.057	6.23

Test Interrupted for Low Level Constant Amplitude Cycling - Loading 1.4 to 6.6 kip

Cycles Elapsed

0	0.089	0.057
8000	0.090	0.057
12000	0.093	0.058
22000	0.094	0.058
37000	0.095	0.058
67000	0.095	0.060 ?*

*Later observations indicate that the readings with a question mark may be in error.

TABLE IV (Contd)

Specimen Cycles Elapsed	2A (inch)	2B (inch)
Low Level Constant Amplitude Cycling 0.3 to 7.7 kip		
0	0.095	0.060?
30,000	0.097	0.061?
100,000	0.098	0.060?
220,000	0.098	0.060?
340,000	0.098	0.062?
465,000	0.098	0.062?
500,000	0.098	0.062?
Truncated Flight-by-Flight Testing Initiated		
Flights Elapsed Program	Flights Elapsed Restart			Percent Lifetime From Restart
755	0	0.098	0.062?	0
800	45	0.098	0.063?	.37
842	87	0.098	0.062?	.72
890	135	0.098	0.062?	1.11
922	167	0.098	0.063?	1.38
970	215	0.098	0.063?	1.77
1022	247	0.100	0.064?	2.04
1050	295	0.100	0.063?	2.43
1082	327	0.100	0.063?	2.70
1130	375	0.098	0.057	3.10
1162	407	0.100	0.058	3.36
1210	455	0.100	0.057	3.75
1242	487	0.101	0.057	4.02
1290	535	0.104	0.058	4.42
1322	567	0.107	0.060	4.68
1370	615	0.110	0.059	5.08
1402	647	0.114	0.060	5.34
1450	695	0.120	0.060	5.74
1482	727	0.125	0.060	6.00
1530	775	0.128	0.060	6.39
1562	807	0.136	0.060	6.66
1610	855	0.140	0.060	7.05
1642	887	0.143	0.060	7.32
1690	935	0.150	0.067*	7.72
1722	967	0.150	0.068	7.98
1770	1015	0.152	0.071	8.38
1802	1047	0.157	0.075	8.64
1840	1095	0.166	0.082	9.04

*Crack extended using B Block repeatedly applied to Specimen 2B placed in parallel with dummy specimen.

TABLE IV (Contd)

Return to Original (Untruncated) Flight-by-Flight Testing				
Specimen Flights Elapsed Program Restart		2A (inch)	2B (inch)	Percent Lifetime From Restart
1840	0	0.166	0.082	0
1850	10	0.173	0.090	0.08
1882	42	0.179	0.090	0.35
1920	80	0.183	0.093	0.66
1962	122	0.190	0.097	1.01
2000	160	0.198	0.104	1.32
2042	202	0.197	0.105	1.67
2090	250	0.202	0.112	2.06
2122	282	0.203	0.115	2.33
2170	330	0.212	0.124	2.72
2202	362	0.219	0.131	2.99
2250	410	0.225	0.137	3.38
2282	442	0.233	0.140	3.65
2314	474	0.240	0.142	3.91
2320	480	0.244	0.145	3.96
Test Interrupted for Low Level Constant Amplitude Cycling 0.3 to 7.7 kip				
Cycles Elapsed				
0		0.244	0.145	
340,000		0.246	0.146	
592,000		0.247	0.147	
815,000		0.247	0.147	
900,000		0.248	0.147	
1,060,000		0.247	0.147	
1,281,000		0.248	0.147	
1,340,000		0.248	0.147	
340,000		0.246	0.147	
815,000		0.247	0.147	
1,340,000		0.248	0.147	
Constant Amplitude Cycling 0.5 to 10. kip				
0		0.248	0.147	
520,000		0.248	0.148	
660,000		0.245	0.145	
720,000		0.245	0.145	
997,000		0.248	0.148	
1,140,000		0.248	0.148	

TABLE IV (Contd)

Constant Amplitude Cycling 0.8 to 12 kip

Specimen Cycles Elapsed	2A (inch)	2B (inch)
0	0.245	0.145
360,000	0.245	0.145

Constant Amplitude Cycling 1 to 15 kip

0	0.245	0.145
75,000	0.244	0.145
105,000	0.244	0.148
127,000	Specimen Cracked to Edge	0.152

Loaded to 57.8 kip, crack in 2B extended abruptly to edge.

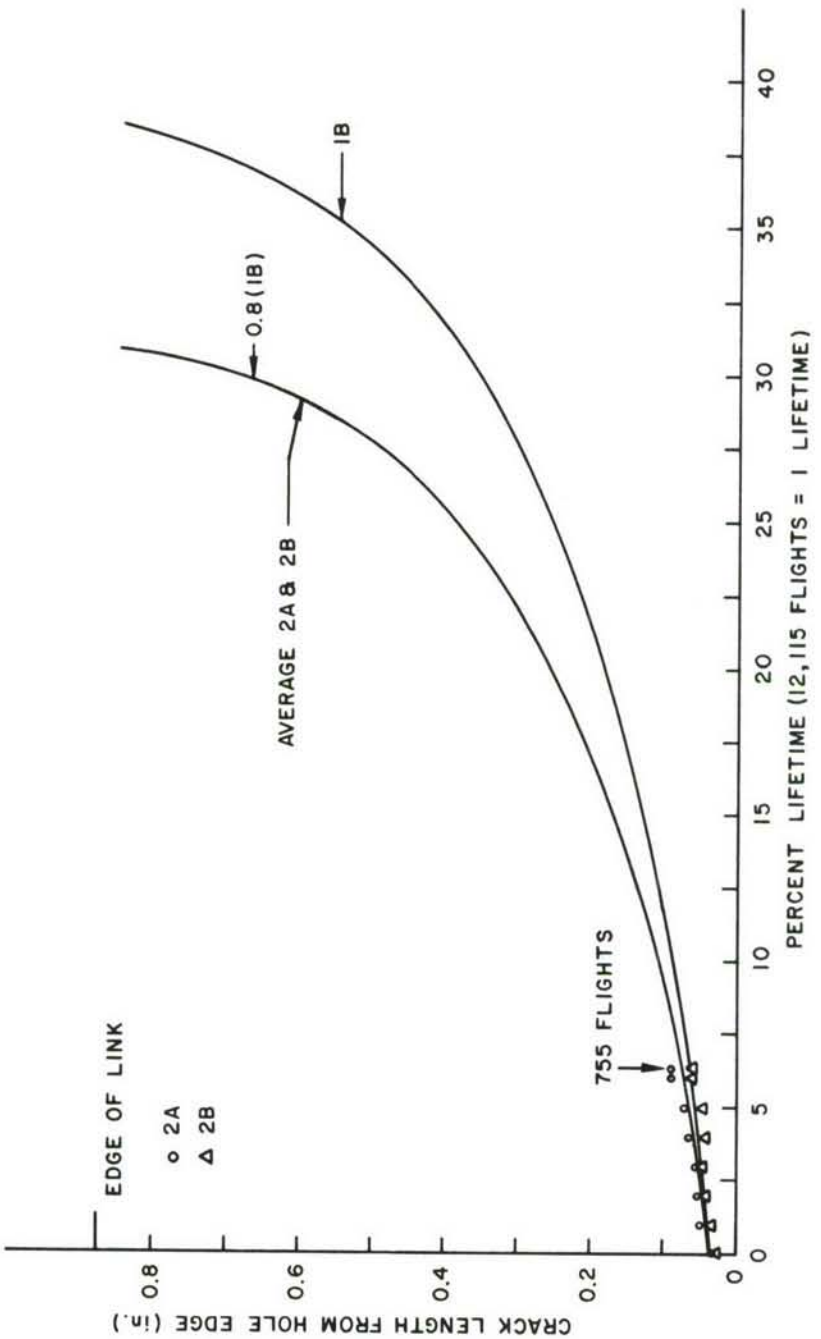

Figure 6. 14-Mission Flight-by-Flight (Untruncated) Spectrum - C-5A Pylon Aft Truss Lug Model

Extensive test time is required to include both GAG load condition 23 and TAG load condition 3 (see Table II), and the contribution of these two conditions (identical load levels but different number of cycles) to crack growth is expected to be insignificant. The flight-by-flight testing was interrupted after 755 flights, therefore, to apply constant amplitude loading to evaluate the influence of the lower level loadings in the test spectrum. Table IV lists the recorded crack length measurements as a function of cyclic change for the constant amplitude conditions given. As can be noted from Table IV, the crack extended 0.009 inch in Link 2A for 567,000 cycles of low-level constant-amplitude cycling (a rate of 1.6×10^{-8} inch/cycle). Using the ratio of load ranges for GAG spectrum load condition 2 (and 23) to that for condition 4 (and 25), as given in Table II, the expected crack growth rate for load condition 2 (and 23) would be approximately three orders of magnitude slower. The growth rate may be even slower if the data in Figure 4 does not extrapolate below 10^{-8} inch/cycle, as we assumed here. Subsequently, a truncated flight-by-flight spectrum (in which GAG load condition 23 and TAG load condition 3 were removed from the original flight-by-flight spectrum) was then applied to Links 2A and 2B.

Figure 7 illustrates the growth behavior of Links 2A and 2B subjected to the truncated flight test spectrum. The crack length at the start of crack movement observed during the truncation test was matched with the identical crack length observed on the 0.8 factor curve from the block spectrum test of Link 1B (see Figure 6) to obtain the corresponding (equivalent) percent lifetime for the continuation of the test. As can be observed from Figure 7, the crack growth behavior continues to extrapolate along the estimated 0.8 factor curve developed from the block spectrum test. Figure 7 also shows that when the truncated spectrum test was discontinued in favor of returning to the untruncated 14-mission flight-by-flight testing, the crack growth behavior continued to extrapolate along the estimated 0.8 block spectrum curve.

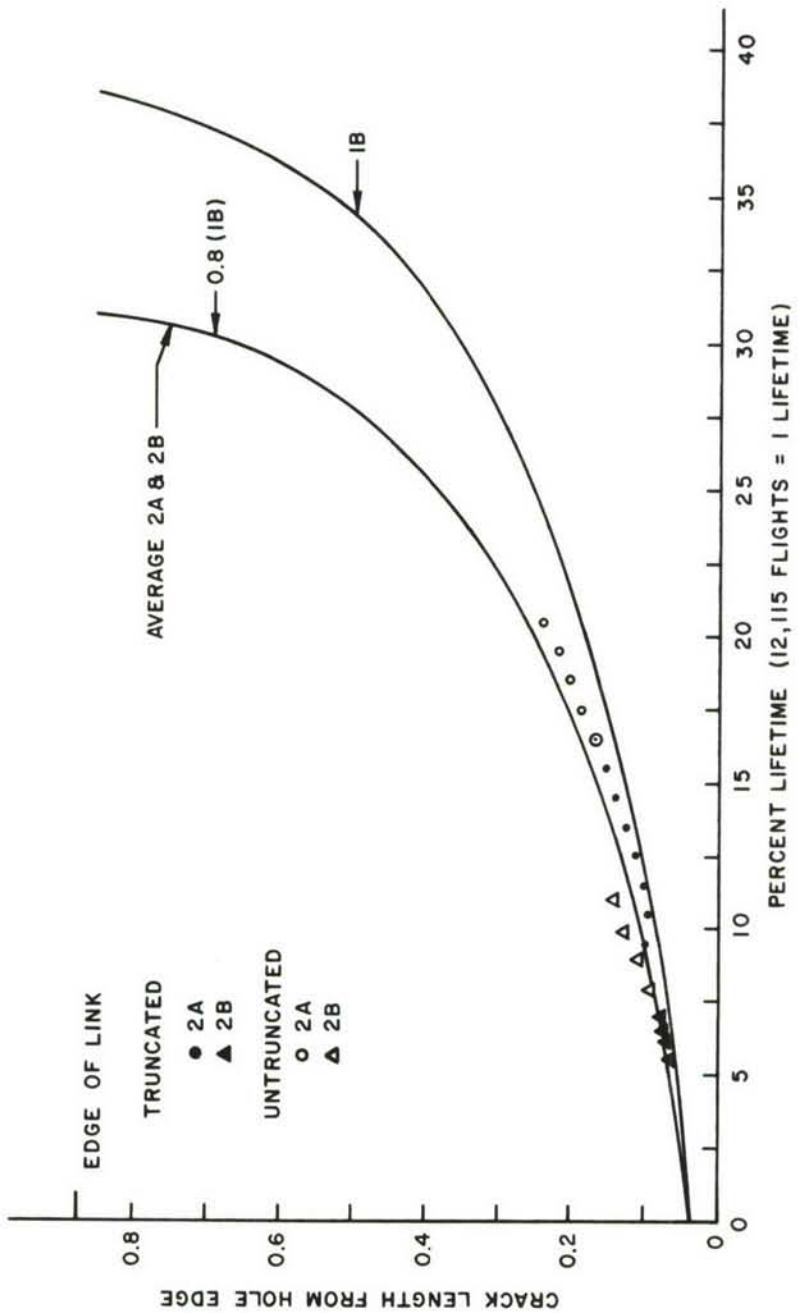

Figure 7. 14-Mission Flight-by-Flight Spectrum -- C-5A Pylon Aft Truss Lug Model

3. COMPARISON OF BLOCK AND FLIGHT-BY-FLIGHT SPECTRA RESULTS

Figure 7 can be used to show directly that the flight-by-flight spectrum produces approximately 25 percent faster crack growth rates than those observed under block loading conditions. Since Figure 7 is plotted on a lifetime basis and since both flight-by-flight and block spectra contain an equal number of GAG cycles, a similar observation on growth rate differences would be observed if Figure 7 were normalized to average extension observed per GAG cycle. Table V lists the principal high load levels associated with block and flight-by-flight spectra. Note that the GAG, TAG, and ERU load levels in the block spectrum are slightly higher than those in the flight-by-flight spectrum. Also note that the block spectrum contains five times more ERU load cycles.

TABLE V

PRINCIPAL HIGH LOAD LEVELS IN BLOCK AND FLIGHT-BY-FLIGHT SPECTRA COMPARED

Spectrum	Condition	Cycles Per Block or Per 16 Flts.	Max. Load kip	Min. Load kip	Cycles in Spectrum Lifetime
Block	GAG	303	37.92	0.2	7575
Block	TAG	178	28.61	0.1	4450
Block	ERU	303	31.18	0.1	7575
Flight	GAG	10	36.8	0	7572
Flight	TAG	6	27.4	0	4343
Flight	ERU	2	31.3	0.1	1514

4. POST FLIGHT-BY-FLIGHT SPECTRUM TESTING

Following the termination of the flight-by-flight testing, a constant amplitude testing program was initiated on Links 2A and 2B. The load levels were chosen from the flight-by-flight load spectrum to determine their influence on the flight-by-flight crack growth behavior. The load levels and the corresponding number of applied load cycles were: 0.3 to 7.7 kip (1,340,000 cycles), 0.5 to 10. kip (1,140,000 cycles), 0.8 to 12.0 kip (360,000 cycles), and 1.0 to 15 kip (127,000 cycles). The three lower levels resulted in no observed growth (less than 0.001 inch), while 105,000 cycles at 1.0 to 15 kip resulted in 0.003 inch growth. An additional 22,000 cycles at this level caused the crack in Link 2A to extend to the edge and a crack movement in Link 2B of 0.004 inch.

5. RESIDUAL LOAD TEST OF CRACKED LINKS

A residual load test of Links 2A and 2B gave a measured maximum load of 57.8 kip which extended the crack in Link 2B from 0.152 inch to the outer edge and almost induced a ductile fracture in the uncracked remaining ligaments of the two links. Proportioning the maximum load so that two-thirds of it was acting on the partially cracked Link 2B (and the remaining one-third on the thru cracked link) resulted in a K_c calculated value of 145 ksi $\sqrt{\text{in}}$ for the fracture of the partially cracked link. The load distribution assumed here was based on the behavior of two strain gaged aluminum links (3A and 3B) which showed equal load distribution until one link cracked to the edge and then a two-to-one load ratio between the partially cracked and fully cracked links. The load was dumped following the abrupt fracture of Link 2B, which precluded the separation of the remaining ligaments.

A strength of materials analysis indicates that a fully ductile fracture of the two remaining uncracked ligaments would be induced by a load of 11 kip, a load well below the maximum loads associated with GAG, TAG, and ERU cycles. The worst case failure that must be anticipated, then, is associated with cracks reaching the outside edge in each of two back-to-back lugs. This analysis verifies the C-5A IRT choice of a two-link worst case condition to test for damage tolerance.

SECTION IV

ANALYSIS OF FLIGHT-BY-FLIGHT LOAD TRUNCATION

1. COMPUTER GENERATED CRACK GROWTH BEHAVIOR

To better determine if truncating the flight-by-flight spectrum affected the results derived from the test, a "Cracks II" computer analysis (Reference 5) of low level load truncation was performed. The Rockwell International crack growth rate data shown in Figure 4 was chosen for this study. These data were adequately described with the following two power law equations:

$$\frac{da}{dn} = 1.321 \times 10^{-11} \Delta K^{4.01}, \quad \text{for } \Delta K \leq 23 \text{ ksi } \sqrt{in} \tag{2}$$

and

$$\frac{da}{dn} = 1.214 \times 10^{-9} \Delta K^{2.56}, \quad \text{for } \Delta K \geq 23 \text{ ksi } \sqrt{in} \tag{3}$$

For each truncation level considered, it was decided to determine increments of crack growth which would occur under an abbreviated but representative flight-by-flight spectrum loading, rather than to work with the whole growth curve. The abbreviated spectrum consisted of the first 16 flights expressed by Equation 1; i.e., the flight-by-flight block was

$$\boxed{F \times F} = 9\boxed{A} + \boxed{B} + 6\boxed{E} \tag{4}$$

where the stresses for the individual flights were obtained by dividing the loads in Table II by 0.664. The stress intensity factor for each stress level was determined using specific stress intensity factor coefficient (K/stress) values. At least six stress intensity factor coefficient values (e.g., 1.3, 1.5, 1.6, 1.8, 2.0, and 2.4 $\sqrt{in}$.) were chosen to span the range of the crack lengths studied in the flight-by-flight tests of the link specimens.

Two spectrum load growth analysis models were employed: (a) a no retardation - no load interaction effect model (conservative) and (b) the Willenborg (AFFDL) (Reference 6) retardation - load interaction accountable model (realistic). The increment of growth which occurred due to the application of the abbreviated flight-by-flight spectrum was obtained by summing the crack growth rates corresponding to the levels of loading, i.e.,

$$\Delta a = \sum_{i=1}^{M} \left.\frac{da}{dN}\right|_i = \sum_{i=1}^{M} f_i\,(\Delta K) \qquad (5)$$

where M represents the total number of load levels in 16 flight-by-flight blocks.

Four truncation conditions were compared: no truncation (full abbreviated block); all loads having a maximum load level below 5.6 kip (8.4 ksi) e.g., GAG loading conditions 2 and 23, TAG loading conditions 1 and 3 (See Table II); all loads having a maximum load level below 9.8 kip (14.8 ksi); and all loads having a maximum load level below 27.4 kip (41.2 ksi). The abbreviated flight-by-flight spectrum, it should be noted, does not sense the influence of the GAG flight, 1 per 100 or 1 per 1000 loads or of the TAG flight 1 per 10, 1 per 100, or 1 per 1000; therefore, the most severely truncated flight-by-flight block eliminates load levels having maximum load levels below 16.2 kip (24.4 ksi).

The incremental growth per abbreviated flight-by-flight block is plotted in Figure 8 as a function of the maximum level of the calculated stress intensity factor (maximum stress, 55.4 ksi x $[K/\sigma]$ values). Figure 8 shows that the fastest rates of cracking are exhibited by the no load interaction model applied to the no truncation block. These cracking rates are approximately a factor of five faster than the retardation-model-developed cracking rates for the same spectrum.

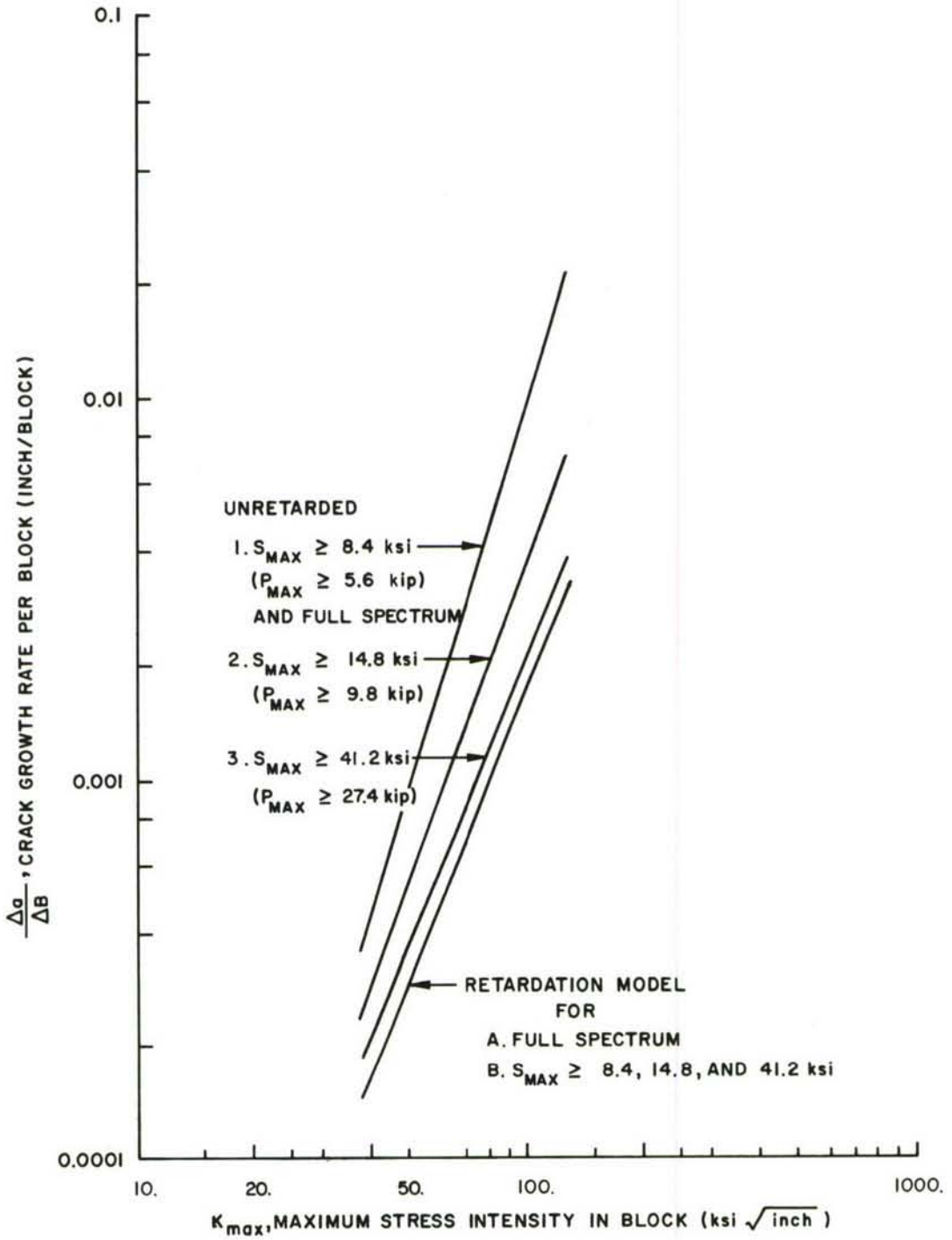

Figure 8. Computer Calculated Crack Growth Increments

All levels of truncation are noted in Figure 8 to give identical growth behavior when the retardation model is used to calculate the incremental growth per block. This implies that the lower level loadings in the 16-flight block introduce no growth because the higher level loads are reducing the low-level-loads effective (crack tip) stress-intensity factors to near zero levels by developing large compressive residual stress levels. As calculated by the retardation model, these lower level stresses would not produce crack growth even if the full 14-mission flight-by-flight spectrum were considered. The closeness of the curve for the most severely truncated no-retardation/no-load-interaction abbreviated flight-by-flight spectrum to that generated by the retardation model reinforces the belief that crack growth, for the most part, is caused primarily by the more frequent higher loads in the spectrum (that is, GAG 1 per 1 condition 22, GAG 1 per 10 condition 1, and TAG 1 per 1 condition 2).

Consideration of the results of the more conservative no-retardation/no-load-interaction model shown in Figure 8 shows that eliminating the lowest load level from both the GAG and TAG flights does not change the growth rate observed under untruncated spectrum conditions. Figure 8 shows that with increasing truncation (additional low load levels deleted), the increments of crack growth per flight-by-flight block decrease.

2. CRACK GROWTH MODEL RESULTS VS. DATA

Figure 7 was used to obtain crack growth rate data which were converted into incremental growth rates for a 16-flight block of the type expressed by Equation 4. These data are presented in Table VI as a function of maximum stress intensity factor for the 16-flight block. Two maximum stress intensity factors were calculated using the maximum stress: one employed the finite element solution (thru-the-thickness crack) (Reference 1), and the other the Anderson-James inverse procedure (Reference 7) (see the Appendix).

TABLE VI

SPECTRUM GENERATED MAXIMUM STRESS INTENSITY FACTOR
VERSUS CRACK GROWTH RATE

Crack Length a (inch)	Kmax Finite Element (ksi $\sqrt{inch}$)	Anderson-James (ksi $\sqrt{inch}$)	$\frac{\Delta a}{\Delta B}$ (inch/block)
0.05	70	50	0.00074
0.10	84	70	0.00123
0.20	93	93	0.00212
0.30	95	107	0.00330
0.40	102	121	0.00475
0.50	110	131	0.00694

Shown in Figure 9 are the computer-calculated crack growth increments which were presented in Figure 8 and the data listed in Table VI. The crack growth data whether expressed using the stress intensity maximum determined by either the Finite Element or the Anderson-James method fall closer to the behavior predicted by the retardation model than to that based on the full-spectrum no-retardation/no-load-interaction model. A log-log trend line through the Anderson-James K_{max} Vs $\frac{\Delta a}{\Delta B}$ data would parallel the model-predicted trends and fall between the unretarded $S_{max} \geq 14.8$ ksi ($P_{max} \geq 9.8$ kip) and $S_{max} \geq 41.2$ ksi ($P_{max} \geq 27.4$ kip) trend lines. A log-log trend line for the finite element determined K_{max} Vs $\frac{\Delta a}{\Delta B}$ data would cut across the computer predicted trends as indicated in Figure 9. If one averaged the stress intensity maximums predicted by the two methods, a log-log trend line through the average K_{max} Vs $\frac{\Delta a}{\Delta B}$ data would be upper bounded by the unretarded $S_{max} \geq 14.8$ ksi ($P_{max} \geq 9.8$ kip) trend line. As reported in the post flight-by-flight spectrum test section of this report, when 360,000 cycles of a 0.8 to 12 kip loading was applied to Links 2A and 2B, no observed crack growth was recorded.

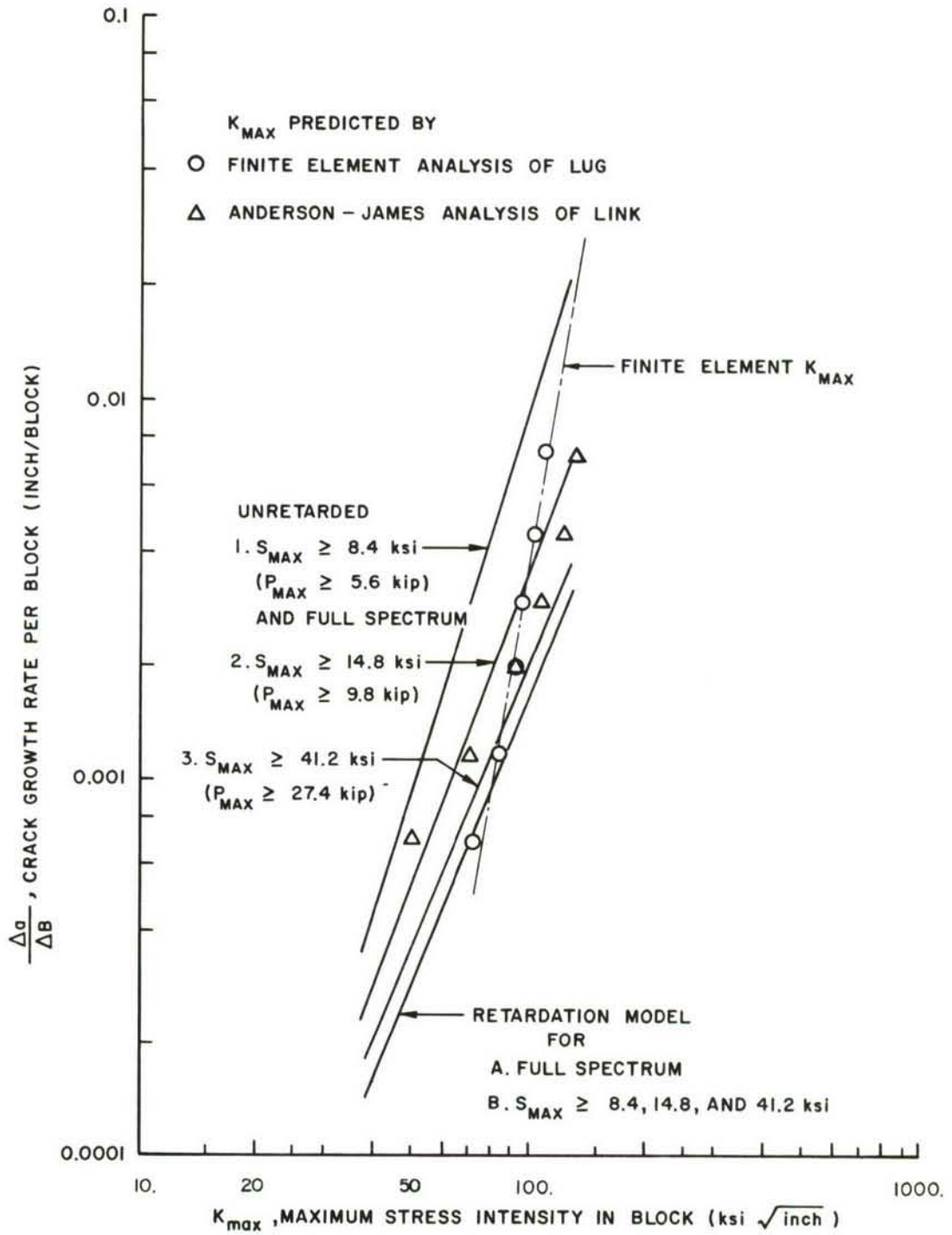

Figure 9. Crack Growth Data Compared to Computer Calculated Crack Growth Increments

For prediction of life or inspection interval, the unretarded $S_{max} \geq 14.8$ Ksi trend line would appear adequate. As suggested by the results discussed in the appendix, the stress intensity factor calibration for the lug should be independently checked so that the crack growth behavior described above can be used in predicting life/inspection interval.

SECTION V

CONCLUSIONS

1. The flight-by-flight spectrum growth rates are 25 percent faster than the rates associated with the block spectrum.

2. The study of lower level load truncation showed that stress levels less than 25 percent of the maximum spectrum stress did not induce fatigue crack growth when the cracks measured less than 0.25 inch from the hole. Therefore, some lower level load levels in the flight-by-flight spectrum could be deleted in any subsequent tests without influencing the growth behavior.

3. Primary growth associated with flight-by-flight and block spectra can be attributed to GAG, ERU, and TAG loadings.

4. If two lugs, back-to-back, are cracked to the edge, an impending failure has to be assumed, since the remaining ligaments cannot withstand GAG level loading.

5. The C-5A-IRT supplied stress intensity coefficient needs to be independently checked for the outboard pylon lug configuration.

6. There does not appear to be any direct correlation between the test results developed during this investigation and the failure of the fatigue test article.

APPENDIX

STRESS INTENSITY FACTOR CALIBRATION

An experimental approach, referred to as the Anderson-James inverse stress intensity factor calibration procedure (Reference 7), was employed to check the finite element stress intensity factor calibration (Reference 1) supplied by the C-5A Independent Review Team. This procedure requires that: (1) the crack growth be measured in a complex geometry where knowledge of the controlling stress intensity factor is lacking; (2) the crack growth be converted to a cyclic crack growth rate as a function of crack length; and (3) that cyclic crack growth rates be established as a function of stress intensity range or maximum by using specimens having known stress intensity factor calibrations. A schematic representation of the steps for finding the stress intensity factor calibration by the inverse procedure for a complex geometry is given in Figure 10.

The GAG cycle induced crack growth data obtained from the block loading spectrum applied to Links 1A and 1B are tabulated in Table VII. These data were supplemented with constant amplitude induced crack growth data obtained from specimens of the same link geometry but which were fabricated from 0.190-inch-thick 7075-T6 aluminum plate stock. The aluminum crack growth data for the test configuration shown in Figure 3B can be found in Table VIII. A test of four aluminum links in the configuration shown in Figure 3C (two sets of cracked-uncracked pairs) resulted in the data listed in Table IX. Figures 11 and 12 show the aluminum crack growth behavior for two cracked link specimens tested in parallel and for two sets of the cracked-uncracked paired link specimens tested in parallel, respectively.

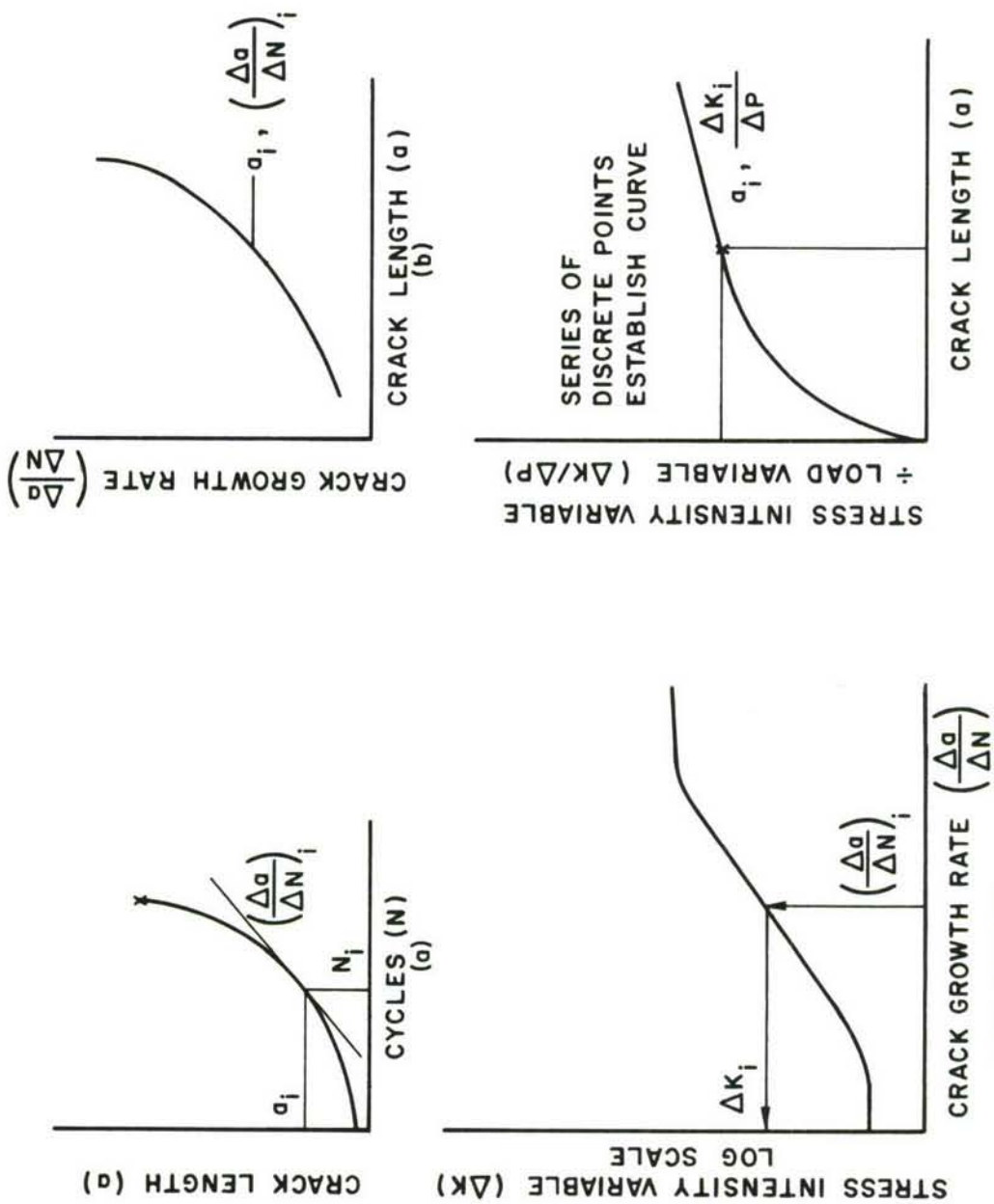

Figure 10. Schematic of Steps Associated with Anderson-James Inverse Procedure

TABLE VII

GAG CYCLE DATA FROM LINK SPECIMENS 1A AND 1B (PH 13-8 Mo)

SPECIMEN	a AVER (in)	Δa (in)	ΔN	$\frac{\Delta a}{\Delta N}$ (10^{-6} in/cycle)	ΔK (ksi $\sqrt{in}$)	ΔP (kip)	$\left(\frac{\Delta K}{\Delta P}\right)^{-3/2}$ (in)
1A	0.105	0.050	303	160	95	37.9	2.5
1A	0.165	0.070	303	230	105	37.9	2.66
1A	0.240	0.030	303	99	79	37.9	2.08
1A	0.285	0.020	303	66	68	37.9	1.79
1A	0.335	0.020	303	66	68	37.9	1.79
1A	0.393	0.016	303	53	62	37.9	1.64
1A	0.480	0.020	303	66	68	37.9	1.79
1A	0.620	0.080	303	265	112	37.9	2.95

SPECIMEN	a AVER (in)	Δa (in)	ΔN	$\frac{\Delta a}{\Delta N}$ (10^{-6} in/cycle)	ΔK (ksi $\sqrt{in}$)	ΔP (kip)	$\left(\frac{\Delta K}{\Delta P}\right)^{-3/2}$ (in)
1B	0.036	0.010	303	33	53	37.9	1.4
1B	0.044	0.005	303	16	39	37.9	1.03
1B	0.058	0.012	303	39	56	37.9	1.48
1B	0.077	0.015	303	49	60	37.9	1.58
1B	0.162	0.034	303	112	82	37.9	2.16
1B	0.215	0.007	303	21	45	37.9	1.19

TABLE VIII

CRACK GROWTH RATE DATA FROM SPECIMENS 4A AND 4B
(7075-T6 ALUMINUM)

SPECIMEN	a Between (in)	a_{aver} (in)	$\frac{da}{dN}$ (10^{-6} in/cycle)	ΔK (ksi $\sqrt{in}$)	ΔP* (kip)	$\frac{\Delta K}{\Delta P}_{-3/2}$ (in)
4A	0.045-0.058	0.052	1.9	5.0	4.29	1.16
4A	0.081-0.118	0.099	4.9	6.8	4.29	1.58
4A	0.120-0.310	0.195	18.5	10.5	4.29	2.45
4A	0.310-0.700	0.505	41.5	14.0	4.29	3.27
4B	0.040-0.065	0.052	3.5	6.1	4.29	1.42
4B	0.070-0.100	0.085	6.4	7.3	4.29	1.7
4B	0.100-0.200	0.150	16.2	10.0	4.29	2.34
4B	0.200-0.400	0.300	41.5	14.0	4.29	3.27

*Stress Ratio R = 0.143

TABLE IX

CRACK GROWTH RATE DATA FROM SPECIMENS 5A AND 5B
(7075-T6 ALUMINUM)

SPECIMEN	a BETWEEN (in)	a_{Aver} (in)	$\frac{da}{dN}$ (10^{-6} in/cycle)	ΔK (ksi $\sqrt{in}$)	ΔP^*_{eff} (kip)	$\frac{\Delta K}{\Delta P}$ $(in)^{-3/2}$
5A	0.15-0.30	0.225	45	14	4.29	3.25
5A	0.240-0.60	0.420	37	13.1	4.29	3.05
5A	0.500-0.68	0.590	39	13.3	4.29	3.1
5A	0.640-0.735	0.690	46	14	4.29	3.25
5B	0.030-0.060	0.045	4.2	6.5	4.29	1.52
5B	0.085-0.150	0.117	13	9.4	4.29	2.18
5B	0.150-0.280	0.215	22	11	4.29	2.56
5B	0.230-0.400	0.315	26	11.8	4.29	2.74
5B	0.360-0.570	0.465	34	12.8	4.29	2.97
5B	0.570-0.720	0.645	50	14.5	4.29	3.38

5A and 5B tested in parallel with two uncracked links

*Stress Ratio R = 0.143

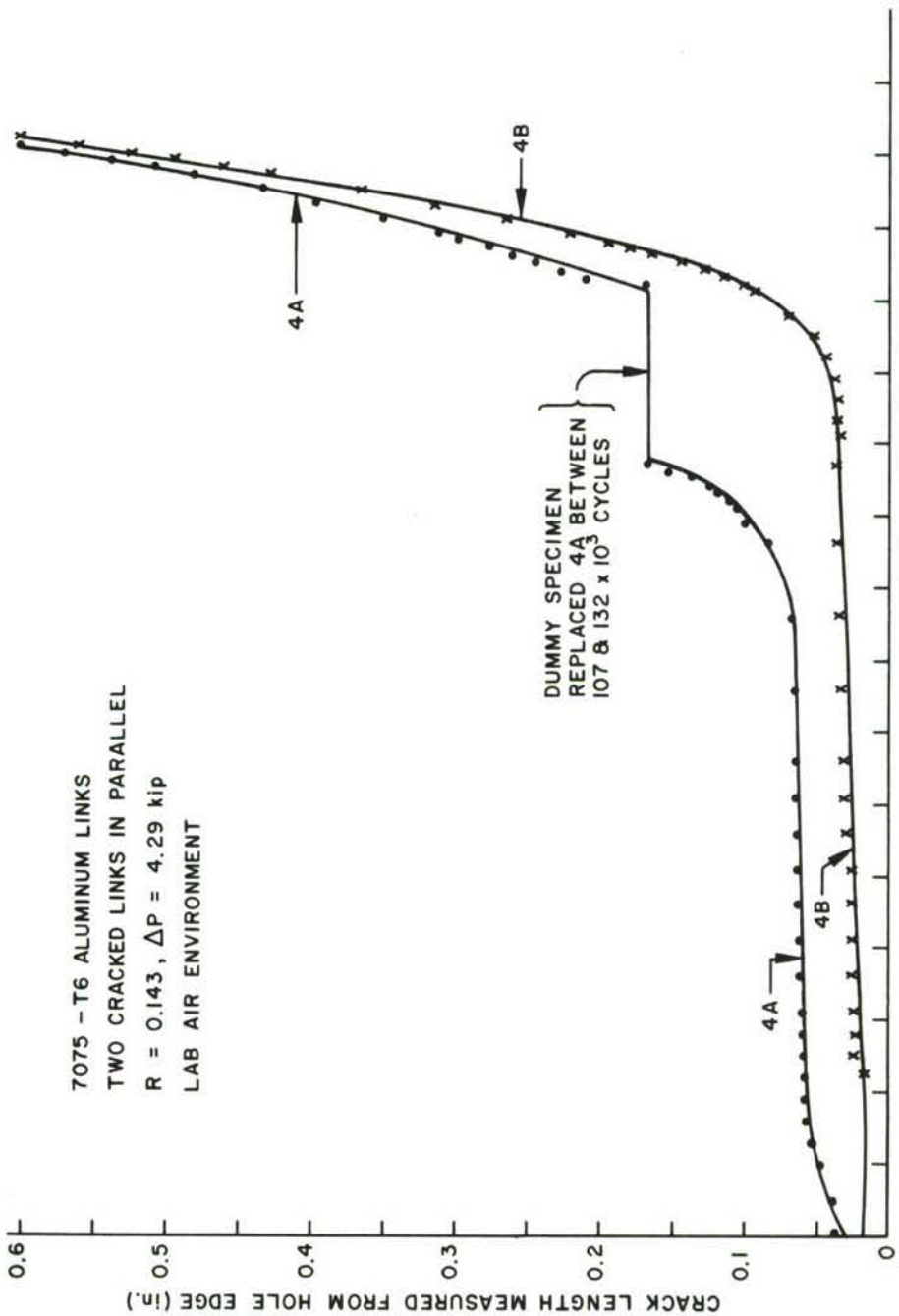

Figure 11. Crack Growth Behavior of Two Aluminum Links Tested in Parallel

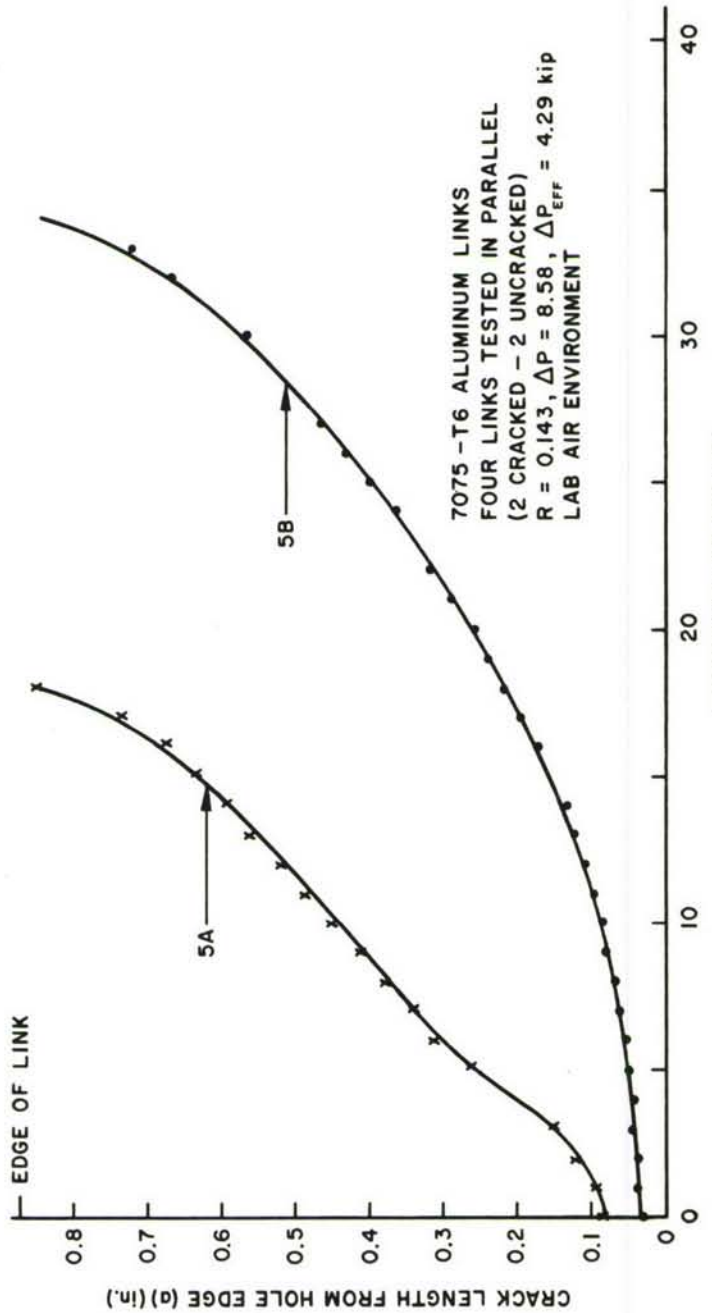

Figure 12. Crack Growth Behavior of Two Cracked Aluminum Links Tested in Parallel with Two Uncracked Aluminum Links

Figure 4 details the PH 13-8 Mo steel crack growth rate behavior as a function of stress intensity range (ΔK) i.e., maximum cyclic stress intensity (K_{max}) minus minimum cyclic stress intensity (K_{min}), while Figure 13 details the behavior for the 7075-T6 stock aluminum. After the inverse procedure was independently applied using the three data sets shown in Figure 4, we decided that the data generated by Rockwell International, the B-1 aircraft contractor, must more accurately reflect the growth behavior of the PH 13-8 Mo steel under the present test condition since it came closest to the results obtained from the aluminum study. Figure 14, which is based on proportionally applied loads to two links, shows coefficient (inverse procedure) data obtained from three tests. W. E. Anderson, consultant to the C-5A SPO, suggested that the aluminum stress intensity coefficient data should be more heavily weighted than the 13-8 Mo steel data since Figure 12 was developed from specimens machined from the same stock as the aluminum link specimens.

Figure 14 shows that for crack lengths less than 0.3 inch, the growth rates associated with the four aluminum links (configuration Figure 3C) tested in parallel are similar to those for two cracked aluminum links tested in parallel; curves which provide a useful approximation to each of the two link tests are given in Figure 14. Figure 15 was developed to compare the results of the two parallel (cracked) link stress intensity factors supplied by the C-5A Independent Review Team (IRT) with that developed for thru-the-thickness type cracks using the Anderson-James procedure. In comparison with the Anderson-James derived curve, the IRT supplied curve is overly conservative at short crack lengths and nonconservative for crack lengths greater than 0.2 inch. It is suggested that an additional independent finite element analysis should be conducted to verify one of these two analyses.

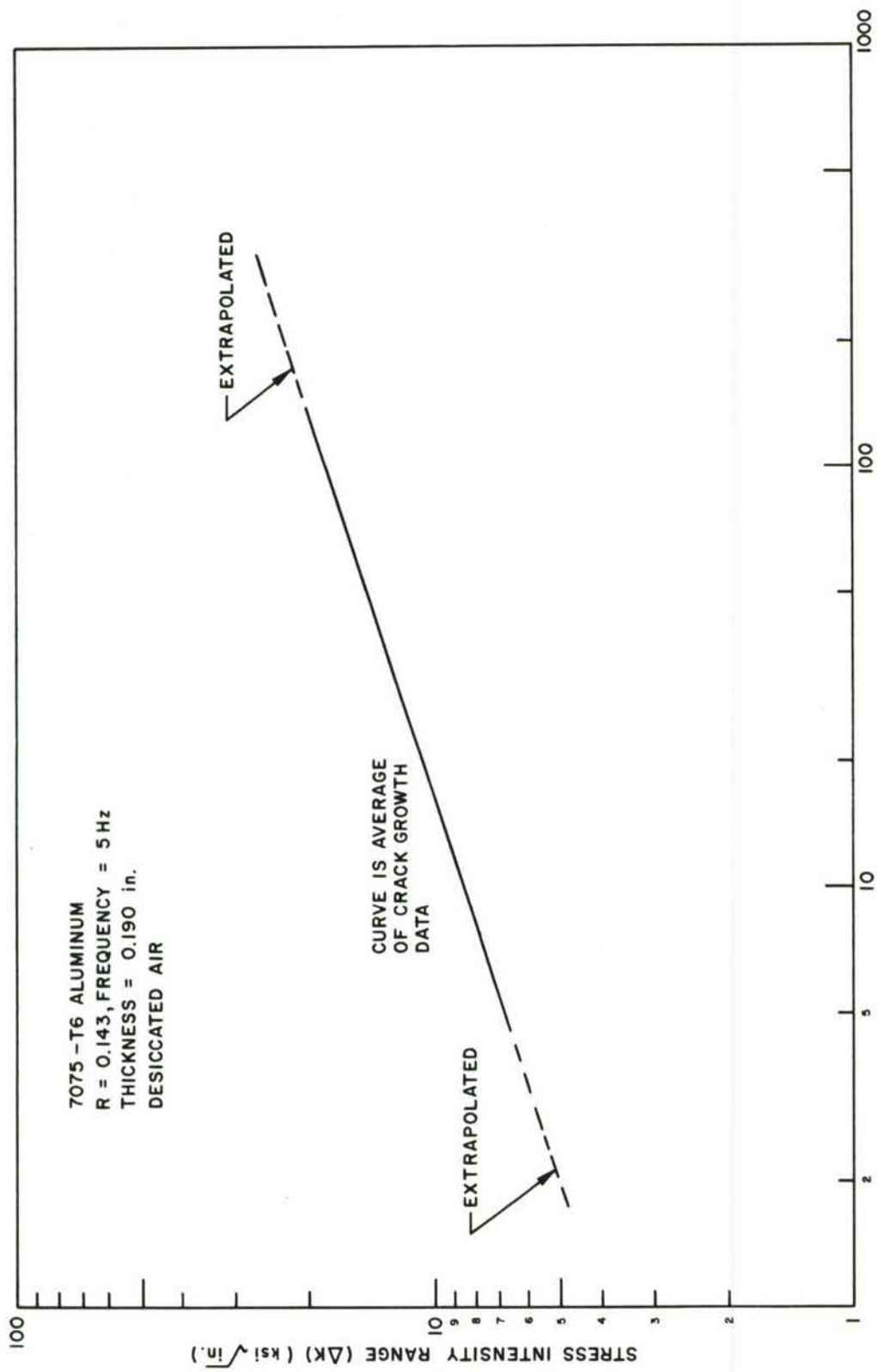

Figure 13. Fatigue Crack Growth Rate Behavior of Stock 7075-T6 Aluminum Alloy

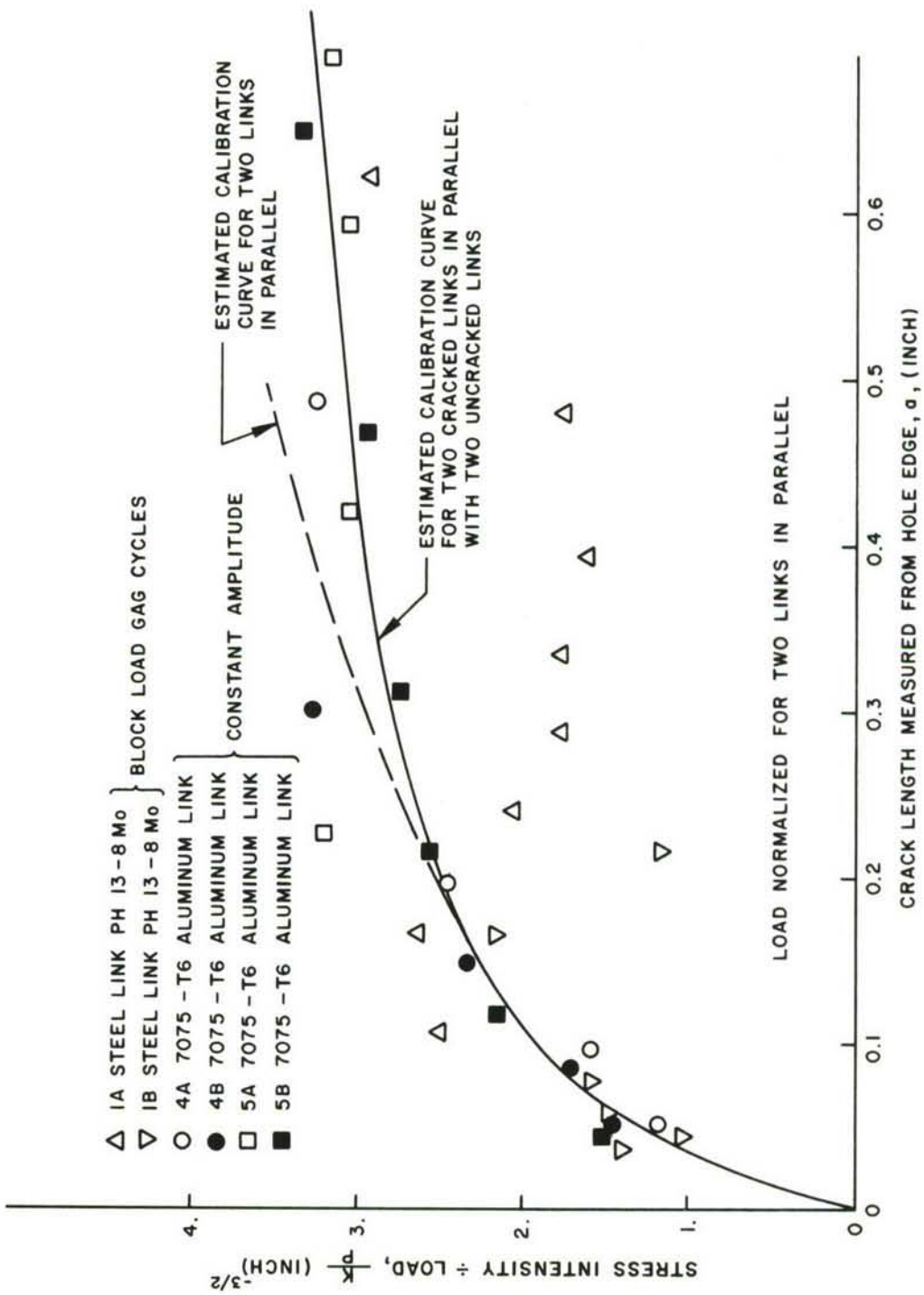

Figure 14. Stress Intensity Factor Coefficients Determined by the Anderson-James Procedure

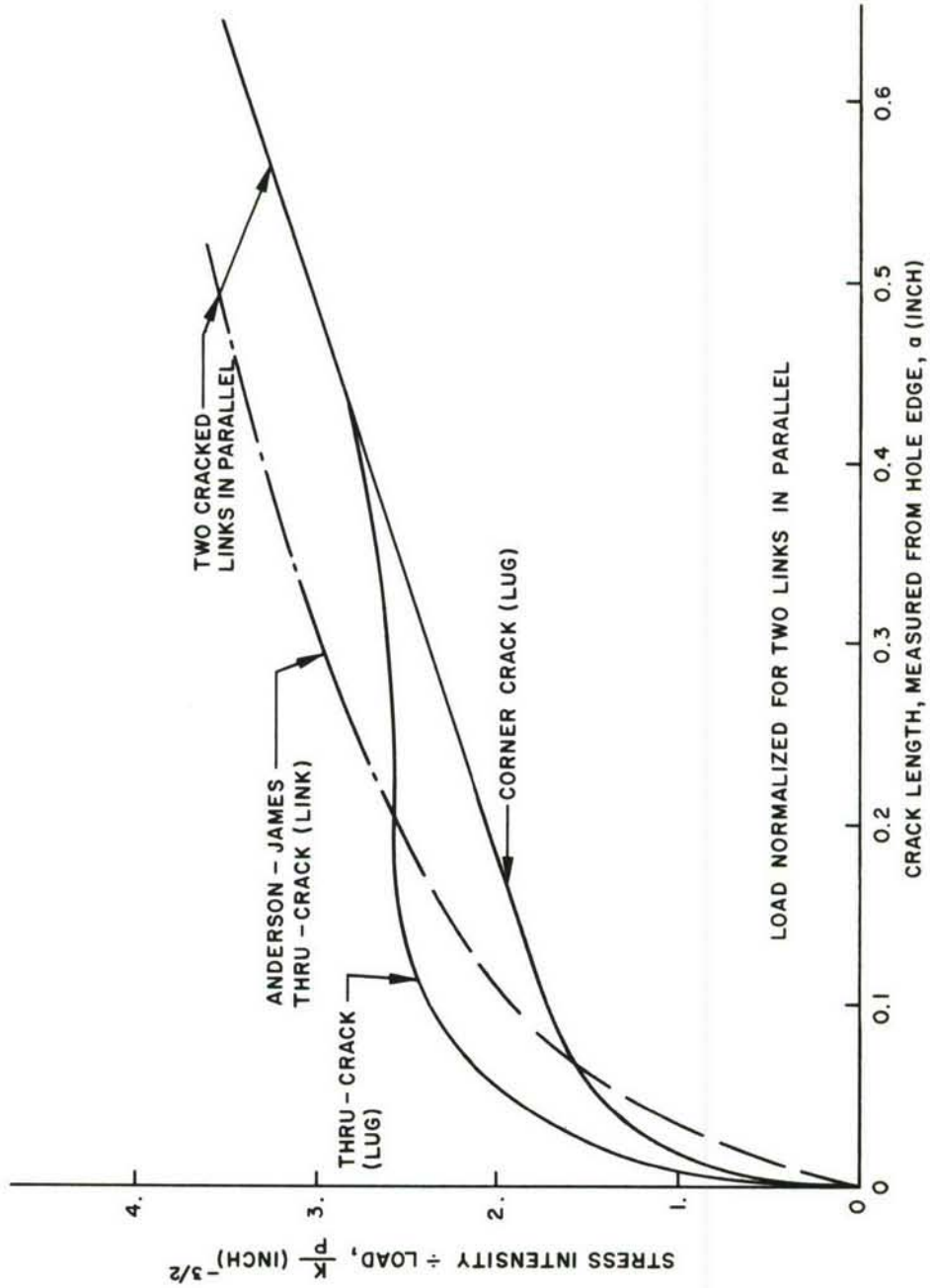

Figure 15. Comparison of Stress Intensity Factor Coefficients

REFERENCES

1. J. M. McKinney, Fracture Analysis: Aft Lug - Pylon Fatigue Test No. 7, M & P Report #14, Lockheed-Georgia Co., Materials and Processes Department (71-11), 15 Nov 1972.

2. Crack Growth Data and Preliminary Report TRM-P supplied in a Private Communication from H. Kirk and R. Goodall to J. P. Gallagher, 19 Dec 1972.

3. Data generated by Rockwell International for B-1 SPO.

4. P. Shahinian, H. E. Watson, and H. H. Smith, "Fatigue Crack Growth in Selected Alloys for Reactor Applications," Journal of Materials, JMLSA, Vol. 7, No. 4, Dec 1972, pp 527-535.

5. R. M. Engle, improved version of computer program reported in Cracks, A FORTRAN IV Digital Computer Program for Crack Propagation Analysis, AFFDL-TR-70-107, October 1970.

6. J. D. Willenborg, R. M. Engle, and H. A. Wood, "A Crack Growth Retardation Model Using an Effective Stress Concept," AFFDL-TM-FBR-71-1, January 1971.

7. L. A. James and W. E. Anderson, "A Simple Experimental Procedure for Stress Intensity Calibration," Engineering Journal of Fracture Mechanics, Vol. 1, No. 3, April 1969, p 565.

☆U.S.Government Printing Office: 1974 — 758-436/728